

# Cathepsin-L Influences the Expression of Extracellular Matrix in Lymphoid Organs and Plays a Role in the Regulation of Thymic Output and of Peripheral T Cell Number<sup>1</sup>

Gabriela Lombardi,\* Dalia Burzyn,\* Juliana Mundiñano,\* Paula Berguer,\* Pedro Bekinschtein,\* Hector Costa,\* Lilian Fedra Castillo,\* Alejandra Goldman,\*<sup>†</sup> Roberto Meiss,<sup>‡</sup> Isabel Piazzon,\* and Irene Nepomnaschy<sup>2\*</sup>

Nackt mice, which are deficient in cathepsin-L (CTSL), show an early impairment during positive selection in the context of class II MHC molecules and as a consequence, the percentage and absolute number of CD4<sup>+</sup> thymocytes are significantly decreased. In this study, we show that lymph nodes from nackt mice are hypertrophied, showing normal absolute numbers of CD4<sup>+</sup> T cells and marked increases in the number of CD8<sup>+</sup> T lymphocytes. Basal proliferative levels are increased in the CD4<sup>+</sup> but not in the CD8<sup>+</sup> population. Lymph node T cells show increases in the expression of  $\alpha_5$ ,  $\alpha_6$ , and  $\beta_1$  integrin chains. These alterations correlate with increases in the expression of extracellular matrix (ECM) components in lymph nodes. Interestingly, laminin, fibronectin, and collagen I and IV are markedly decreased in nackt thymus which shows an augmented output of CD8<sup>+</sup> cells. These results demonstrate that a mutation in the *Ctsl* gene influences the levels of ECM components in lymphoid organs, the thymic output, and the number of T cells in the periphery. They further raise the possibility that, by regulating the level of expression of ECM components in lymphoid organs, CTSL is able to broadly affect the immune system. *The Journal of Immunology*, 2005, 174: 7022–7032.

Cells in lymphoid tissues are surrounded by a web of extracellular matrix (ECM)<sup>3</sup> glycoproteins, which contribute to the determination of the particular tissue microenvironment and its functional characteristics. During intrathymic maturation, thymocytes interact with cellular and noncellular stromal thymic components. Thymic ECM is not restricted to the basal membranes, but is also heterogeneously distributed in the thymic interstitium forming a thick network in the medullary region of the thymic lobules, whereas very thin ECM fibers are found within the cortex (1, 2). In lymph nodes, ECM components are abundant in the interfollicular compartments but they are poorly expressed in both primary and secondary follicles (3). In addition to their mechanical role, ECM glycoproteins are important signaling molecules with the ability to strongly influence thymocyte and lymphocyte programs, promoting differentiation, migration, proliferation, and activation (4–9). Moreover, different growth

factors, chemokines, and hormones are associated with ECM, this association being an important factor in regulating cellular responsiveness (10–14).

The lysosomal cysteine peptidase cathepsin-L (CTSL), an abundant and ubiquitously expressed member of the papain family that contributes to the terminal degradation of proteins in the lysosome, can also be secreted (15). There is accumulating evidence for specific functions of CTSL and other lysosomal proteases in health and disease (16–22). The use of “knockout” (KO) or mutant mice deficient in CTSL has provided a valuable tool for gaining new insights into the in vivo functions of this protease (21–27).

In mice, CTSL has been shown to be critical for epidermal homeostasis, the regulation of the hair cycle (18, 23), and the maintenance of the heart structure and function (24). A role for CTSL in trophoblast invasion (17), tumor metastasis (16), thyroid function (25), and mammary gland involution (19) has also been demonstrated. CTSL plays an important role in the MHC class II-mediated peptide presentation in thymic epithelial cells, acting both in Ii degradation (21) and in the generation of MHC class II-bound peptide ligands presented by cortical thymic epithelial cells (22). Nakagawa et al. (21) reported that CTSL is critical for degradation of Ii in cortical epithelial cells and as a consequence, CTSL KO mice exhibit a marked reduction in the percentage of CD4<sup>+</sup> cells in the thymus and the periphery. We have shown that nackt (*nkt/nkt*) mice—which carry a mutation in the *Ctsl* gene (26)—have an early impairment during positive selection of CD4 thymocytes (27). In this study, we report that *nkt/nkt* mice show hypertrophied lymph nodes, which have normal absolute numbers of CD4<sup>+</sup> cells and marked increases in the number of CD8<sup>+</sup> lymphocytes. Whereas the normalization in the number of lymph node CD4<sup>+</sup> cells correlates with increases in basal proliferative levels, increases in CD8<sup>+</sup> cells correlate with a significant increase in thymic export of these T cells. Interestingly, the thymus and lymph nodes of *nkt/nkt* mice show opposite alterations in the expression levels of ECM glycoproteins.

\*Instituto de Leucemia Experimental (ILEX)-Consejo Nacional de Investigaciones Científicas y Técnicas (CONICET), División Medicina Experimental, Instituto de Investigaciones Hematológicas, <sup>†</sup>Escuela de Ciencia y Tecnología, Universidad Nacional de San Martín, and <sup>‡</sup>Instituto de Estudios Oncológicos, Academia Nacional de Medicina, Buenos Aires, Argentina.

Received for publication April 19, 2004. Accepted for publication March 25, 2005.

The costs of publication of this article were defrayed in part by the payment of page charges. This article must therefore be hereby marked *advertisement* in accordance with 18 U.S.C. Section 1734 solely to indicate this fact.

<sup>1</sup> This work was supported by grants from CONICET, L-Agencia para la Promoción Científica y Tecnológica (ANPCYT)-Fundación para Combatir la Leucemia (FUNDALEU).

<sup>2</sup> Address correspondence and reprint requests to Dr. Irene Nepomnaschy, División Medicina Experimental, Instituto de Investigaciones Hematológicas, Academia Nacional de Medicina, Pacheco de Melo 3081(1425) Buenos Aires, Argentina. E-mail address: irenepo@hematologia.anm.edu.ar

<sup>3</sup> Abbreviations used in this paper: ECM, extracellular matrix; CTSL, cathepsin-L; KO, knockout; Cy, CyChrome; RTE, recent thymic emigrant; PI, propidium iodide; SP, single positive; IGF, insulin growth factor; IGFBP, IGF binding protein; DP, double positive.

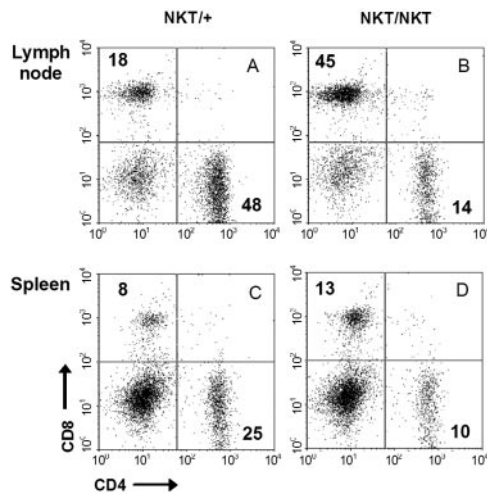


**FIGURE 1.** Alterations in cell subsets in the lymph nodes and spleen of *nkt/nkt* mice. Lymphocytes from lymph nodes (A and B) or spleen (C and D) of *nkt/nkt* mice (B and D) and *nkt/+* littermates (A and C) were stained with anti-CD4 and anti-CD8 and analyzed by FACS. Dot plots depict representative results from three different experiments. Percentages of CD4<sup>+</sup> and CD8<sup>+</sup> cells are indicated in each quadrant.

## Materials and Methods

### Mice

As described in a previous paper (28), the *nkt* mutant allele arose in the laboratory animal facilities of the Martin-Luther-Universität (Halle-Wittenberg, Germany) in a stock derived from irradiated founder no. 372 of the late P. Hertwig. At the Pasteur Institute they were crossed to 129/Sv/Pas inbred breeders for a few generations, then intercrossed. Mice segregating for *nkt* were transferred to the animal facilities of our laboratory where the mutant allele was backcrossed onto a BALB/c background by performing 10 successive rounds of cross/intercross (N10). Specific pathogen-free *nkt/nkt* and *nkt/+* littermates were used. BALB/c mice were produced and maintained in our animal facility. The mice were housed according to the policies of the Academia Nacional de Medicina (National Institutes of Health Guide for the Care and Use of Laboratory Animals). *nkt/nkt* mutants were identified by their alopecia; the presence of one, two, or no copies of the deletion in *Ctstl* gene was detected by RT-PCR (sense primer 5'CAATCAGGGCTGTAACGGAGG 3', antisense primer 5'CAT-TGAGGATCCAAGTCATG3'). Total cellular RNA from thymus was isolated using an RNeasy Mini kit (Qiagen), and first-strand cDNA was synthesized using cloned Avian Myeloblastosis Virus Reverse Transcriptase (Invitrogen Life Technologies) according to the manufacturer's protocols. cDNA was amplified by PCR using the following conditions: 50 s at 94°C, 50 s at 60°C, 50 s at 72°C, and a final elongation step of 10 min at 72°C.

### Monoclonal Abs

The following mAbs conjugated to FITC, PE, or CyChrome (Cy) were used for flow cytometric analysis (all from BD Pharmingen): anti-CD4 (clone H129.19); anti-CD8a (clone 53-6.7); anti-CD69 (clone H1.2F3); anti-CD44 (clone IM7), anti-CD49d (clone R1-2), anti-CD49e (clone 5H10-27 (MFR5)), anti-CD49f (clone GoH3), anti-CD29 (clone Ha2/5), anti-TCR $\beta$  (clone H57-597).

### Cell suspensions

Single cell suspensions of lymphocytes were prepared from a pool of four axillary and two inguinal lymph nodes as previously described (29). This pool of lymph nodes was used to calculate the number of cells per lymph node. Mononuclear cells from spleen were isolated by centrifugation on Ficoll-Trioyson gradients.

### Flow cytometric staining

For double or triple staining, lymphocytes from lymph nodes or spleen ( $10^6$  cells), resuspended in RPMI 1640 without phenol red (Invitrogen Life Technologies) containing 3% FBS (Invitrogen Life Technologies), 0.1% sodium azide, and 10 mM HEPES (Invitrogen Life Technologies), were incubated in one step with the appropriate mAbs (27). Acquisition of 30,000 cells (or 100,000 cells for recent thymic emigrant (RTE) experiments) was done using a FACScan flow cytometer (BD Biosciences) appropriately set-up for two- or three-color fluorometry. Dead cells were excluded on the basis of forward- and side-cell scatter. Background values obtained with fluorochrome conjugate isotype controls (BD Pharmingen) were subtracted. Results were analyzed using Cell Quest software (BD Immunocytometry Systems).

### Histology and immunohistochemistry

Thymus and lymph nodes were removed and fixed in 10% neutral-buffered formalin. Sections were processed routinely and embedded in paraffin. Each sample was stained with H&E. Immunohistochemistry was performed using the streptavidin-biotin-peroxidase complex system LSAB (DAKO). Endogenous peroxidase activity was blocked by 3% hydrogen peroxide in methanol for 5 min and Ag retrieval was performed by microwaving. Following preblocking with normal serum, tissue slides were incubated overnight with the following primary Abs: polyclonal rabbit anti- $\alpha$  laminin (AB19012) (Chemicon International); polyclonal rabbit anti- $\alpha$  fibronectin (H-300); polyclonal goat anti- $\alpha$  collagen I (M-19) or polyclonal rabbit anti- $\alpha$  collagen IV (H-234) from Santa Cruz Biotechnology. These incubations were followed by incubation with biotinylated anti-rabbit or anti-goat Abs. Sections were incubated with a streptavidin-horseradish-peroxidase complex. The peroxidase reaction was conducted using diaminobenzidine. Omission of the primary Ab or replacement with an irrelevant Ab during staining gave a negative result in every case. Sections were analyzed by a Zeiss Axiophot2 microscope. For semiquantitative analysis, the level of immunohistochemical staining was rated as high, moderate, low, or not detectable (3, 2, 1, and 0, respectively). Five mice per experimental group were analyzed; scoring was done blindly by two independent scorers and the results averaged for each sample. For quantitative assessment of immunohistochemical staining in the thymus, images were captured using a Cool SNAP-pro color camera (Media Cybernetics). Images were collected from five control and mutated mice. Multiple digital images were captured and color segmentation was performed to highlight the stained area. Image-Pro Plus software was used to calculate the number of pixels positively stained on each image, and this value was expressed as a percentage of the total area. Care was taken to ensure that images were obtained from consistent regions (medullary or cortical areas of the thymus). Image analysis was performed on coded, randomized sections by a blinded observer.

### ECM Western blot analysis

Proteins were extracted from frozen lymph nodes ( $-70^{\circ}\text{C}$ ) homogenized in lysis buffer (10 mM Tris-HCl (pH 7.6)/5 mM EDTA/50 mM NaCl/30 mM  $\text{Na}_4\text{P}_2\text{O}_7$ /50 mM NaF/200  $\mu\text{M}$   $\text{Na}_3\text{VO}_4$ /1% Triton X-100/1 mM PMSF/5  $\mu\text{g/ml}$  aprotinin/1  $\mu\text{g/ml}$  pepstatin A/2  $\mu\text{g/ml}$  leupeptin) using a Polytron. Then the samples were incubated for 1 h at  $-20^{\circ}\text{C}$ . The supernatant was

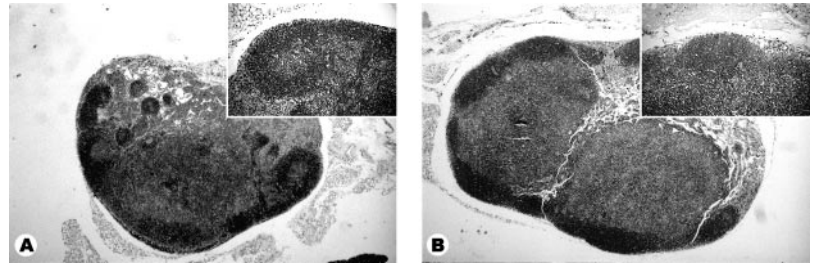
Table I. Alterations in cell subsets in the lymph nodes and spleen of *nkt/nkt* mice<sup>a</sup>

	Absolute Number ( $\times 10^{-6}$ )					
	Lymph node			Spleen		
	CD8 <sup>+</sup>	CD4 <sup>+</sup>	B220 <sup>+</sup>	CD8 <sup>+</sup>	CD4 <sup>+</sup>	B220 <sup>+</sup>
<i>nkt/+</i>	1.7 $\pm$ 0.6	4.3 $\pm$ 1.5	1.9 $\pm$ 0.9	6.9 $\pm$ 2.6	18.5 $\pm$ 1.8	139.5 $\pm$ 10.6
<i>nkt/nkt</i>	9.9 $\pm$ 1.7*	4.0 $\pm$ 0.9	5.2 $\pm$ 2.1*	20.2 $\pm$ 6.3*	8.0 $\pm$ 3.0*	167.3 $\pm$ 40.1

<sup>a</sup> Lymphocytes from lymph nodes and spleen from *nkt/nkt* mice and *nkt/+* littermates were stained with anti-CD8, anti-CD4, and anti-B220 and analyzed by FACS. Values represent the mean of total number  $\pm$  SD ( $n = 4$ ).

\*,  $p < 0.01$  compared to *nkt/+*. The experiment was performed three times with similar results.

**FIGURE 2.** *nkt/nkt* lymph nodes show alterations in the histological structure. *A*, Lymph node from *nkt/+* with normal cortical and paracortical areas (H&E,  $\times 25$ ); *inset*, follicular structure in paracortical area (H&E,  $\times 250$ ). *B*, *nkt/nkt* lymph node with subcapsular compressed follicles and enlarged paracortical area (H&E,  $\times 25$ ); *inset*, subcapsular protruded follicle of packed lymphoid cells (H&E,  $\times 250$ ).



kept after centrifugation at 13,000 rpm for 30 min at 4°C. Protein extracts (0.1 mg) were resuspended in 2 $\times$  sample buffer (250 mM Tris-HCl (pH 6.8)/4% SDS/10% glycerol/2% 2-ME/0.006% bromphenol blue), boiled for 3 min, centrifuged briefly, and fractionated on an SDS 6 or 8% polyacrylamide gel. Proteins were transferred overnight onto polyvinylidene difluoride membranes using a Bio-Rad Western blot apparatus. For Western blot analysis, blots were blocked overnight with PBS with 0.1% Tween 20 (PBST) plus 5% nonfat dried milk (v/v) at room temperature for 2 h. Blots were incubated overnight at 4°C with the primary Ab diluted in PBST/3% BSA. Antiserum was diluted 1/400 for type IV collagen (Santa Cruz Biotechnology) and 1/200 for laminin (Sigma-Aldrich). After three washes in PBST, peroxidase-conjugated goat anti-rabbit IgG (Santa Cruz Biotechnology) was diluted to 1/25,000 and incubated for another 2 h at room temperature. After three additional washes in PBST, protein levels were analyzed by ECL detection system (Amersham Pharmacia Biotech). Subsequently, membranes were washed and immunoblotted with anti- $\beta$  actin to check the protein load in each lane. The intensity of ECM protein levels was quantified using the NIH image program. To calculate the relative abundance of mutant band it was normalized to that obtained with control mice. Western blot analysis for CTSL was conducted according to standard protocols (30) and visualized by ECL detection kits (Amersham Pharmacia Biotech). Ab against mouse cathepsin L (R&D Systems) was diluted to 1/500. Anti-goat HRP (Santa Cruz Biotechnology) was diluted to 1/500 and incubated for 1 h at 37°C.

#### FITC labeling of thymocytes and quantification of migrant populations in host mice

Thymocyte labeling was done as previously described by Berzins et al. (31). Briefly, mice were anesthetized and after opening the thorax cavity, each thymic lobe was injected with 10  $\mu$ l of 500  $\mu$ g/ml FITC in PBS. This injection typically resulted in random labeling of 30–70% of thymocytes. Mice were killed  $\sim$ 20 h after injection and lymphoid organs were removed for analysis. Only animals with >50% of FITC<sup>+</sup> thymocytes were included in experimental groups. Samples were stained with anti-CD4 Cy and anti-CD8 PE, then analyzed by flow cytometry. Emigrant cells were identified as live-gated FITC<sup>+</sup> cells expressing either CD4 or CD8. The absolute numbers of FITC<sup>+</sup> CD4<sup>+</sup> and FITC<sup>+</sup> CD8<sup>+</sup> cells among live-gated cells were added to provide the total emigrant number for lymph nodes (pooled from mesenteric, inguinal, axillary, and popliteal lymph nodes) and spleen. These data were used for calculation of the total number of cells exported from the injected thymus in the previous 24 h. RTE numbers in the periphery were corrected based on the proportion of labeled thymocytes using the formula: corrected RTE = measured RTE/ $x$ , where  $x$  = % FITC<sup>+</sup> thymocytes.

#### Proliferation

Lymphocytes from lymph node or spleen ( $2 \times 10^6$  cells), resuspended in PBS (without Ca<sup>2+</sup> and Mg<sup>2+</sup>) containing 3% FBS (Invitrogen Life Technologies), were incubated in with FITC-conjugated anti-CD4 or anti-CD8. The cells were washed in cold PBS and resuspended in 1 ml of ethanol 70% and stored 18 h at 4°C. Cells were washed and resuspended in 500  $\mu$ l of staining solution (1 mg/ml RNase A (Sigma-Aldrich), 20  $\mu$ g/ml propidium iodide (PI; Sigma-Aldrich)) in PBS containing 1g/L glucose and incubated for 30 min. Acquisition of 30,000 cells was done using a FAC-Scan flow cytometer.

#### Data presentation

Except where specified, the figures and tables contain representative results from experiments repeated independently three times. The animals were always tested individually.

#### Statistics

The two-tailed Student *t* test or the Mann-Whitney *U* test were used to assess the statistical significance of the results. A value of  $p < 0.05$  was considered indicative of a significant difference.

## Results

### Alterations in T cell populations in peripheral lymphoid organs from *nkt/nkt* mice

We have previously reported that the positive selection of CD4<sup>+</sup> cells is impaired in the thymus of *nkt/nkt* mice, thus showing a considerable decrease in the percentage and absolute number of CD4<sup>+</sup> single-positive (SP) thymocytes (27). Herein we investigated whether these mice showed alterations in peripheral lymphoid organ T cells. The spleen of *nkt/nkt* mice showed normal cellularity. The percentage and the absolute number of CD4<sup>+</sup> cells

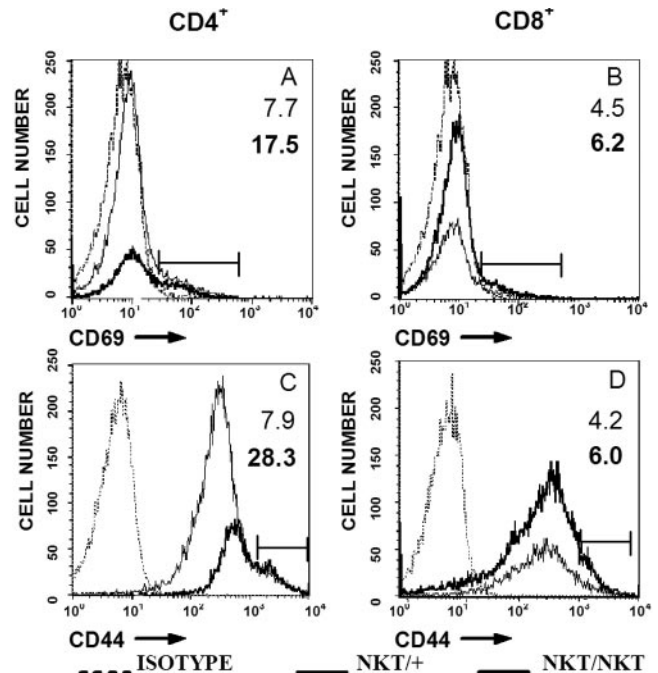


**FIGURE 3.** *nkt/nkt* mice show increases in the percentage of CD4<sup>+</sup> lymph node cells expressing activation/adhesion markers. Expression of CD69 (*A* and *B*) and CD44 (*C* and *D*) on CD4<sup>+</sup> (*A* and *C*) and CD8<sup>+</sup> (*B* and *D*) T cells from lymph nodes of *nkt/nkt* or *nkt/+* mice was analyzed by FACS. The percentages of CD69<sup>+</sup> and CD44<sup>high</sup> cells in the CD4<sup>+</sup> and CD8<sup>+</sup> gates are indicated for *nkt/+* or *nkt/nkt*. Similar numbers of total lymph node cells were analyzed for the wild-type and the mutant samples. *A* and *C*, The lower value of the histograms of the *nkt/nkt* samples reflects the decrease in the percentage of CD4<sup>+</sup> cells, as previously described; *B* and *D*, the higher values of the histograms of *nkt/nkt* samples reflect the increase in the percentage of CD8<sup>+</sup> cells. Histograms depict representative results from five independent experiments.

Table II. *nkt/nkt* mice show alterations in the expression of adhesion/activation markers on CD4<sup>+</sup> and CD8<sup>+</sup> T cell subsets in the periphery<sup>a</sup>

	Lymph node				Spleen			
	CD8 <sup>+</sup>		CD4 <sup>+</sup>		CD8 <sup>+</sup>		CD4 <sup>+</sup>	
	CD44 <sup>high</sup>	CD69 <sup>+</sup>	CD44 <sup>high</sup>	CD69 <sup>+</sup>	CD44 <sup>high</sup>	CD69 <sup>+</sup>	CD44 <sup>high</sup>	CD69 <sup>+</sup>
	Experiment no. 1							
<i>nkt/+</i>	3.4 ± 1.0	3.0 ± 1.8	8.3 ± 1.3	7.0 ± 3.5	22.5 ± 9.5	2.8 ± 0.8	13.3 ± 0.1	6.0 ± 1.0
<i>nkt/nkt</i>	6.8 ± 2.5	4.9 ± 1.5	24.9 ± 3.7***	15.2 ± 3.6*	28.6 ± 8.7	1.8 ± 0.9	25.6 ± 2.9**	5.8 ± 0.7
	Experiment no. 2							
<i>nkt/+</i>	3.9 ± 0.8	2.8 ± 1.5	9.0 ± 1.1	8.2 ± 2.3	25.3 ± 5.3	3.3 ± 1.2	15.2 ± 1.4	4.3 ± 0.8
<i>nkt/nkt</i>	5.0 ± 1.4	5.2 ± 0.6	22.5 ± 3.0***	18.5 ± 2.6**	23.9 ± 3.7	2.2 ± 1.3	20.3 ± 2.2**	3.6 ± 1.1
	Experiment no. 3							
<i>nkt/+</i>	6.1 ± 1.1	2.8 ± 1.6	10.7 ± 0.9	6.5 ± 1.9	30.2 ± 6.4	2.2 ± 0.5	17.5 ± 3.0	4.9 ± 1.2
<i>nkt/nkt</i>	5.6 ± 1.3	4.5 ± 1.9	26.3 ± 2.2***	12.6 ± 2.16**	27.7 ± 3.9	1.3 ± 0.7	25.2 ± 3.8*	6.3 ± 0.9

<sup>a</sup> Lymphocytes from lymph nodes and spleen of *nkt/nkt* mice and *nkt/+* littermates were stained with anti-CD44 or anti-CD69 and anti-CD4 or anti-CD8 and analyzed by FACS. Values represent the mean percentages of CD44<sup>high</sup> and CD69<sup>+</sup> gated on CD4<sup>+</sup> and CD8<sup>+</sup> cells ± SD ( $n = 4$ ). \*,  $p < 0.02$ , \*\*,  $p < .01$ , \*\*\*,  $p < 0.001$  compared to *nkt/+*. Three of five experiments with similar results are shown.

were significantly decreased whereas the number of CD8<sup>+</sup> cells was increased (Fig. 1 and Table I). Lymph nodes were hypertrophied ( $17.1 \times 10^6 \pm 5.1$  ( $n = 22$ ) total lymphocytes per lymph node in *nkt/nkt* mice vs  $6.0 \times 10^6 \pm 3.2$  ( $n = 15$ ) in *nkt/+* mice,  $p < 0.001$  (mean ± SD)). The histological examination of lymph nodes showed that the overall structure was modified by: 1) the presence in the upper cortex of compressed subcapsular follicle-like structures without germinal centers, mostly composed of small, dark-stained lymphoid cells; 2) an enlarged paracortical area that seems to compress the cortical areas and projects deeply into the medulla; 3) a medullary area with dilated sinuses with macrophages and medullary cords variable in size and shape, composed by darkly stained and loosely arranged lymphoid cells (Fig. 2).

As can be observed in Fig. 1 and Table I, although the percentage of CD4<sup>+</sup> T cells was decreased in *nkt/nkt* lymph nodes, their absolute number was not significantly different from that of *nkt/+* mice. The percentage and absolute number of CD8<sup>+</sup> T cells in *nkt/nkt* lymph nodes was markedly increased. The absolute number of B220<sup>+</sup> lymph node cells was also found to be increased in *nkt/nkt* mice (Table I).

Concerning the expression of activation/adhesion molecules, the percentage of CD44<sup>high</sup> and CD69<sup>+</sup> cells within CD4<sup>+</sup> lymph node cells was found to be significantly increased in *nkt/nkt* mice. A 3-fold increase in the percentage of CD4<sup>+</sup> cells expressing high levels of CD44 and a 2-fold increase in the percentage of cells expressing CD69 was consistently recorded in mutant mice (Fig. 3 and Table II). In the spleen, CD4<sup>+</sup> cells showed a significant increase in the percentage of CD44<sup>high</sup> cells whereas the percentage of CD69<sup>+</sup> cells remained unchanged (Fig. 3). CD8<sup>+</sup> cells did not show significant differences in the expression of CD44 or CD69 molecules either in lymph nodes or in the spleen (Table II).

#### CD4<sup>+</sup> lymphocytes from lymph nodes of *nkt/nkt* mice show a significant increase in their basal proliferative level

To investigate whether cell proliferation was involved in the alterations observed in lymphoid organs of *nkt/nkt* mice, lymphocytes were stained with PI and FITC-conjugated anti-CD4 or anti-CD8 Abs. As can be shown in Fig. 4, *A* and *B*, the percentage of proliferating CD4<sup>+</sup> lymph node cells was significantly higher in *nkt/nkt* than in *nkt/+* mice ( $0.6 \pm 0.2$  vs  $2.7 \pm 0.6$  in *nkt/nkt* mice ( $n = 4$ ),  $p < 0.01$  (mean ± SD)). No increases in proliferative levels were found in CD4<sup>+</sup> *nkt/nkt* splenocytes ( $0.6 \pm 0.2$  vs  $0.5 \pm 0.3$ , NS). CD8<sup>+</sup> cells showed normal proliferative levels both in the spleen ( $0.9 \pm 0.3$  vs  $0.8 \pm 0.2$ ) and in lymph nodes ( $0.8 \pm 0.1$  vs  $0.6 \pm 0.2$ ) (Fig. 4, *C* and *D*).

No differences in the level of apoptosis of CD4<sup>+</sup> and CD8<sup>+</sup> cells from lymph nodes could be detected as assessed by PI incorporation (CD4<sup>+</sup> cells:  $0.91 \pm 0.23$  vs  $0.86 \pm 0.16$ ); CD8<sup>+</sup> cells:  $0.78 \pm 0.3$  vs  $0.81 \pm 0.22$ , in *nkt/+* vs *nkt/nkt* mice, NS (mean % ± SD) ( $n = 4$ )). Similar results were obtained when the level of apoptosis of CD4<sup>+</sup> and CD8<sup>+</sup> splenocytes was recorded (data not shown).

#### Lymph nodes from *nkt/nkt* mice show increases in ECM components

Immunohistochemical studies showed that the expression of ECM glycoproteins was significantly increased in lymph nodes of *nkt/nkt* mice as assessed by semiquantitative analysis. Fibronectin expression was moderately increased in the follicular areas and highly increased in interfollicular areas, fibrous capsule, sinuses, and vessels. Fibronectin was also strongly expressed in epithelial cells (Fig. 5, *A* and *B*). Expression of laminin was higher in the

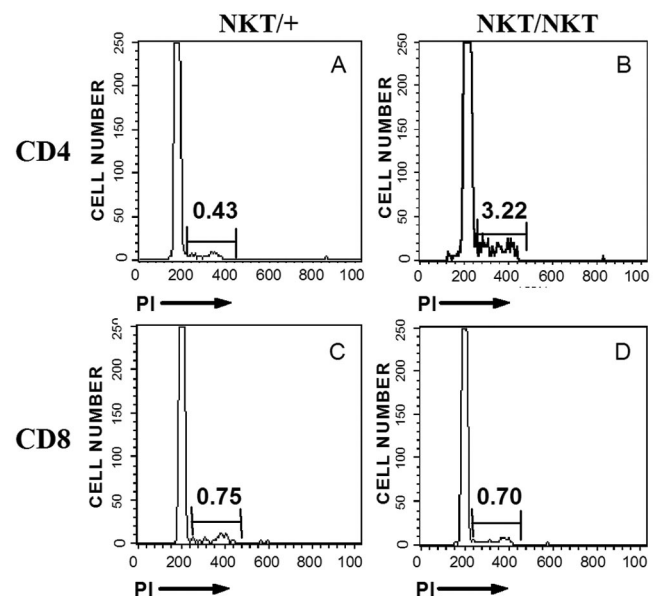


**FIGURE 4.** CD4<sup>+</sup> T cells from lymph nodes of *nkt/nkt* mice show an increase in their basal proliferative level. Lymphocytes from lymph nodes of *nkt/+* (*A* and *C*) or *nkt/nkt* mice (*B* and *D*) were stained with anti-CD4 or anti-CD8 and PI and analyzed by FACS. Percentages of basal proliferative level are indicated. Histograms depict representative results from three independent experiments.

interfollicular areas, in the fibrous capsule, and in vessels (Fig. 5, C and D). It was also highly expressed in sinuses and epithelial cells. For collagen type I, *nkt/nkt* mice show a moderate and diffuse expression in the cortical area, with higher intensity in the fibrous capsule (Fig. 5, E and F). *nkt/nkt* mice show a moderate and diffuse expression of collagen type IV in the parenchyma, with higher intensity in fibrous capsule (Fig. 5, G and H). Increases in the expression of laminin and collagen IV in lymph nodes were confirmed using Western blot assays (Fig. 6). No differences in the expression of these ECM components in the spleen of *nkt/nkt* mice were observed (Fig. 6).

*nkt/nkt* mice show increases in the percentage of lymph node  $CD4^+$  and  $CD8^+$  cells expressing high levels of  $\alpha_5$ ,  $\alpha_6$ , and  $\beta_1$  integrin chains

The expression of integrin chains in lymph node T cells from *nkt/nkt* and *nkt/+* mice was investigated using cytofluorometric techniques. A 2- to 3-fold increase in the percentage of  $CD4^+$  and  $CD8^+$  cells expressing high levels of  $\alpha_6$ ,  $\alpha_5$ , and  $\beta_1$  integrin chains was consistently observed (Fig. 7 and Table III). No differences in the level of expression of these integrin chains was observed in  $CD4^+$  or  $CD8^+$  splenocytes from *nkt/+* and *nkt/nkt* mice (Table III).

The rate of  $CD8^+$  thymic emigrants is increased in *nkt/nkt* mice

To investigate whether the thymic export was involved in the alterations observed in the peripheral T cell pool of *nkt/nkt* mice,

animals were intrathymically injected with FITC and the recent thymic emigrant (RTE) cells were identified as live-gated  $FITC^+$  cells expressing either  $CD4$  or  $CD8$  molecules in the periphery 24 h later. As can be observed in Table IV, the total number of  $CD4^+$  RTE exported daily to the periphery was significantly smaller in *nkt/nkt* than in *nkt/+* mice whereas the total number of  $CD8^+$  RTE exported was increased more than 2-fold in *nkt/nkt* mice.

The rate of thymic export was calculated as the relation of peripheral  $FITC^+CD8^+$  or  $FITC^+CD4^+$  RTE/total  $CD8^+$  or  $CD4^+$  SP thymocytes, respectively (31). Whereas the rate of thymic export of  $CD4^+$  cells was not significantly different in *nkt/nkt* vs control mice, a 3-fold increase in the rate of export of  $CD8^+$  thymocytes was observed in *nkt/nkt* mice (Table IV). These data suggest a direct role of augmented thymic output of  $CD8^+$  cells in the increase of this lymphoid population registered both in lymph nodes and in spleen from mutant mice.

Taking into account that the level of expression of CD69 on the cell surface changes from high in the less mature SP cells to negative just before SP thymocytes exit this organ (32, 33), the expression of this marker on  $CD8^+$  SP was investigated. No differences in the level of expression of CD69 were detected in the  $CD8$  thymic compartment when thymocytes from *nkt/nkt* and *nkt/+* mice were compared (Fig. 8). These data suggest that changes in the speed of maturation and exit included all the stages because neither diminution nor accumulation in any specific stage of SP maturation could be detected.

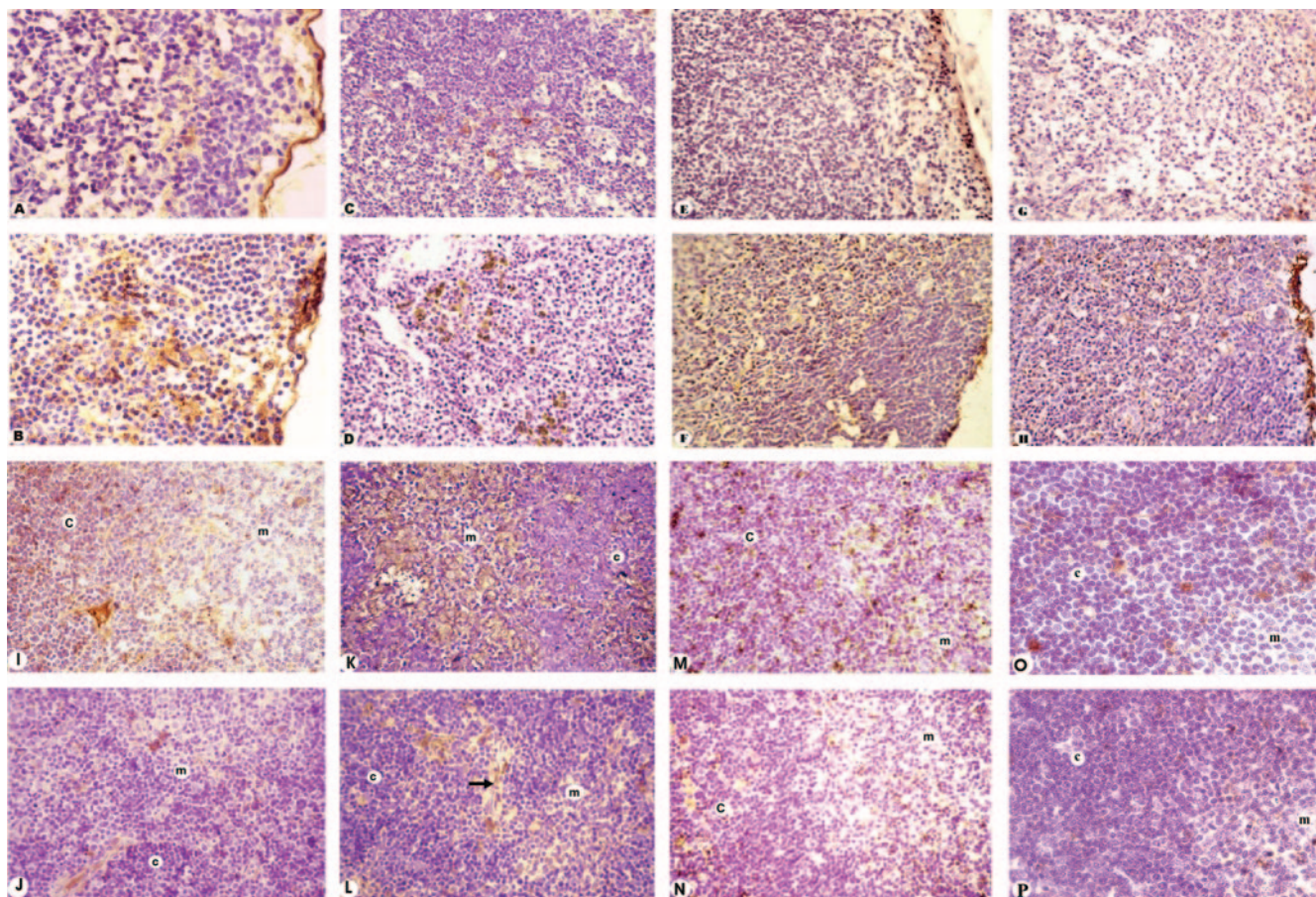


**FIGURE 5.** Alterations in the expression of ECM in lymph nodes and thymus of *nkt/nkt* mice. Lymph nodes of *nkt/+* (A, C, E, and G) and *nkt/nkt* (B, D, F, and H) mice were immunostained for: fibronectin (A and B;  $\times 400$ ); laminin (C and D;  $\times 250$ ); collagen type I (E and F;  $\times 250$ ) and collagen type IV (G and H;  $\times 250$ ). Thymi from *nkt/+* (I, K, M, and O) and *nkt/nkt* (J, L, N, and P) mice were immunostained for: fibronectin (I and J;  $\times 250$ ); laminin (K and L: note the low expression of laminin in the perivascular space (arrow)) ( $\times 250$ ); collagen type I (M and N;  $\times 250$ ) and collagen type IV (O and P;  $\times 400$ ).

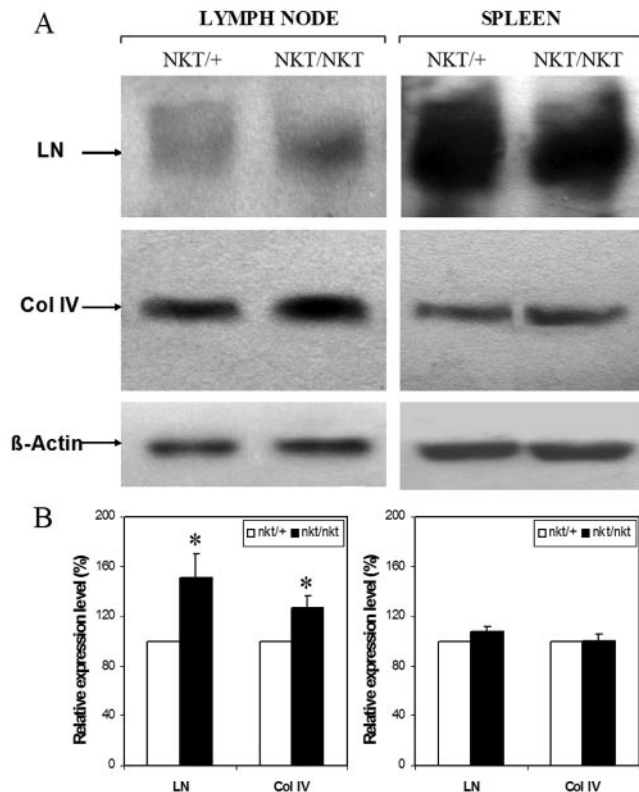


**FIGURE 6.** *nkt/nkt* mice show increases in ECM protein levels in lymph nodes. *A*, Western blot analysis of protein extracted from *nkt/+* and *nkt/nkt* mice immunoblotted with anti-laminin (LN), anti-collagen type IV (Col IV), anti- $\beta$  actin. *B*, Quantification of the results in lymph node and spleen of three independent mice. Each column and bar of *nkt/nkt* mice represents the mean and SD of the percentages obtained when each blot was compared with *nkt/+*. \*,  $p < 0.01$ .

*The thymus of nkt/nkt mice shows decreases in ECM components*

In a conventional histological study, the thymus from *nkt/nkt* mice showed a loss of the basic lobular pattern mainly due to a diminished septa thickness (Fig. 9). A normally vascularized corticomedullary junction showed an ill-defined boundary. The corticomedullary relation was altered with clear predominance of the cortex. Less packed thymocytes were found in the outer cortex. To investigate the expression of thymic ECM glycoproteins, immunohistochemical studies were conducted. A significant decrease in the level of expression of fibronectin, laminin, and collagen I and IV was observed not only in the medulla but also in the cortex in mutant mice. As can be observed in Fig. 5, *I* and *J*, the decrease of fibronectin expression was observed in epithelial cells, basal membranes, and perivascular spaces. Fibronectin was minimally expressed in the capsula/septa. A general decrease in laminin expression was also observed in the thymus from *nkt/nkt* mice. A very marked decrease was observed in the medullar area and in epithelial cells. (Fig. 5, *K* and *L*). The expression of collagen I (Fig. 5, *M* and *N*) and collagen VI (Fig. 5, *O* and *P*) was also diminished. A weak stain for collagen IV was observed in both the cortical and the medullar network and also in some scattered epithelial cells as well as in capsula/septa and perivascular space. The expression of collagen I showed a general diminution. Thymocytes were negative for all the ECM components studied. Staining for ECM components was analyzed by image analysis both in the cortex and medulla. A significant decrease in the cortical staining was observed in *nkt/nkt* mice (laminin:  $8.1 \pm 0.5$  vs  $5.5 \pm 0.6$ ; fibronectin:

$8.2 \pm 0.9$  vs  $1.9 \pm 0.7$ ; collagen IV:  $2.2 \pm 0.3$  vs  $0.23 \pm 0.22$ ; collagen I:  $5.2 \pm 1.0$  vs  $1.2 \pm 0.5$ , expressed as mean percentage of the stained area  $\pm$  SEM ( $n = 5$ ). In the medulla, levels of ECM components were also shown to be significantly lower in *nkt/nkt* mice (laminin  $11.6 \pm 0.9$  vs  $4.2 \pm 0.6$ ; fibronectin:  $11.4 \pm 1.1$  vs  $2.6 \pm 0.9$ ; collagen IV:  $2.24 \pm 0.3$  vs  $1.2 \pm 0.16$ ; collagen I:  $4.9 \pm 1.3$  vs  $0.78 \pm 0.3$ ). Overall, these data indicate a clear decrease in the main components of ECM in the thymus of *nkt/nkt* mice.

*Expression of integrins in thymocytes from nkt/nkt mice*

The expression of integrin chains during the different stages of thymocyte differentiation determined by the level of expression of the TCR $\beta$  chain was investigated. No differences in the level of expression of  $\alpha_4$ ,  $\alpha_5$ , and  $\alpha_6$  (Fig. 10 and Table V) and  $\beta_1$  (not shown) integrin chains along the different stages of T cell maturation could be detected.

*nkt/nkt mice express a mutated CTSL*

Thymus and skin extracts from *nkt/nkt* and *nkt/+* mice were subjected to Western blot analysis using the AF1515 Ab (R&D Systems) directed to aa 18–334 of recombinant mouse CTSL. This Ab was able to detect the characteristic pattern of bands corresponding to pre-pro, pro, and mature forms of CTSL in tissue extracts from *nkt/+* mice. Although with less intensity, a similar pattern of bands was observed in tissue extracts from *nkt/nkt* mice (Fig. 11).

**Discussion**

We had previously described that *nkt/nkt* mice, which have a deletion in the *Ctst* gene (26), showed an early impairment during

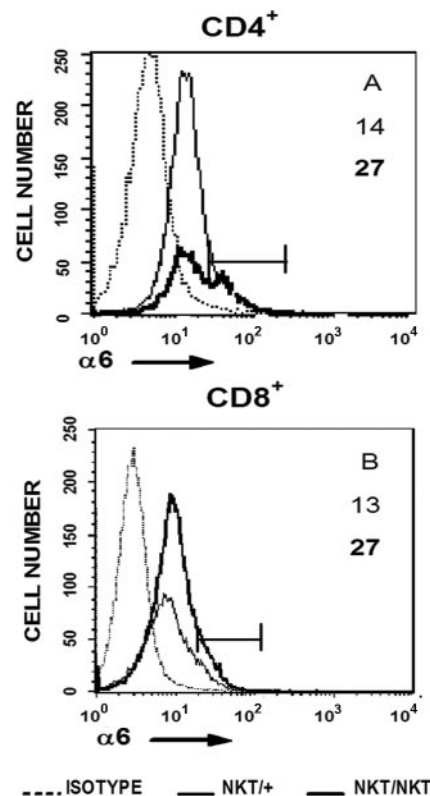


**FIGURE 7.** Lymph node from *nkt/nkt* mice show increases in the expression of the  $\alpha_6$  integrin chain on T cells. Expression of the  $\alpha_6$  integrin chain on CD4<sup>+</sup> (*A*) and CD8<sup>+</sup> (*B*) T cells from lymph nodes of *nkt/nkt* mice or *nkt/+* was analyzed by FACS. Percentages of  $\alpha_6^{\text{high}}$  are indicated for *nkt/+* or *nkt/nkt*. Histograms depict representative results from three independent experiments.

Table III.  $\alpha_6$ ,  $\alpha_5$ , and  $\beta_1$  integrin chain expression in T lymph node and spleen cells from *nkt/nkt* mice<sup>a</sup>

	Lymph Node						Spleen					
	CD4 <sup>+</sup>			CD8 <sup>+</sup>			CD4 <sup>+</sup>			CD8 <sup>+</sup>		
	$\alpha_6$	$\alpha_5$	$\beta_1$	$\alpha_6$	$\alpha_5$	$\beta_1$	$\alpha_6$	$\alpha_5$	$\beta_1$	$\alpha_6$	$\alpha_5$	$\beta_1$
<i>nkt/+</i>	12.8 ± 2.6	7.6 ± 1.9	16.5 ± 1.4	12.4 ± 1.3	4.0 ± 0.9	9.3 ± 1.1	11.4 ± 1.9	6.9 ± 1.7	15.7 ± 1.6	16.0 ± 1.9	5.7 ± 1.2	10.3 ± 2.4
<i>nkt/nkt</i>	<b>27.4 ± 4.3</b>	<b>22.5 ± 1.3</b>	<b>36.3 ± 3.0</b>	<b>36.2 ± 3.7</b>	<b>10.9 ± 1.3</b>	<b>23.9 ± 1.5</b>	13.1 ± 3.5	8.3 ± 1.9	13.8 ± 2.4	14.4 ± 1.7	4.9 ± 1.5	11.9 ± 1.2

<sup>a</sup> Lymph node or splenocytes from *nkt/+* and *nkt/nkt* littermates were stained with anti-CD4 or anti-CD8 and anti-CD49e, anti-CD49f or anti-CD29 and analyzed by flow cytometry. Values represent the mean percentages of cells expressing high levels of  $\alpha_6$ ,  $\alpha_5$  or  $\beta_1$  integrin chains ± SD ( $n = 4$ ) within within CD4<sup>+</sup> and CD8<sup>+</sup> subsets. Bold values, significantly different from *nkt/+* ( $p < 0.01$ ). The experiment was performed three times with similar results.

positive selection in the context of major class II MHC molecules (27). Consequently, the percentage and absolute number of CD4<sup>+</sup> SP thymocytes were significantly decreased. No differences in the percentage and absolute number of SP CD8<sup>+</sup> thymocytes could be registered.

In this study, we show that peripheral lymph nodes of *nkt/nkt* mice are enlarged, showing a 2- to 3-fold increase in cell number. Histologically, the most remarkable features were compressed subcapsular follicle-like structures without germinal centers and an enlarged paracortical area that projects deeply into the medulla. The overall structure seems to correspond to a hyperplastic non-reactive lymph node. Accordingly, the numbers of B and T cells in *nkt/nkt* lymph nodes were significantly increased. The number of CD4<sup>+</sup> cells was similar to that of normal littermates. This subpopulation of T cells displayed a significant overrepresentation of cells with an activated/memory phenotype—based on the expression of CD44 and CD69 molecules—and an increased basal proliferative level. The percentage and absolute number of CD8<sup>+</sup> cells were markedly increased. Differently from results registered in the CD4<sup>+</sup> population, the CD8<sup>+</sup> subset showed a normal proportion of cells with an activated/memory phenotype and a normal basal proliferative level. In the spleen, which shows normal cellularity, the number of CD4<sup>+</sup> cells was decreased whereas CD8<sup>+</sup> cells were found to be highly increased. The same phenotypic characteristics (i.e., increases in lymph node cellularity, in the number of CD8<sup>+</sup> lymph node cells and in CD4<sup>+</sup> proliferative levels along with higher numbers of CD4<sup>+</sup> cells expressing high levels of CD44) were observed in *nkt/nkt* mice backcrossed on C57BL/6J.

The number of CD4<sup>+</sup> cells leaving the thymus daily was found to be diminished in *nkt/nkt* mice and their thymic export rate—as suggested in a previous report (27)—was not significantly altered when compared with *nkt/+* littermates. On the contrary, both the number of CD8<sup>+</sup> cells leaving the thymus daily and the CD8<sup>+</sup> thymic export rate were significantly increased in mutant mice.

These data show that the marked increment in the number of CD8<sup>+</sup> peripheral cells correlates with increases in CD8<sup>+</sup> thymic output. The low number of CD4<sup>+</sup> T cells in the spleen correlates with the decrease in CD4 thymic output. In contrast, in lymph nodes, the mechanisms by which *nkt/nkt* mice reach normal numbers of CD4<sup>+</sup> cells involve increases in cell proliferation.

Lysosomal cystein peptidases of the papain family exhibit high collagenolytic (34) and elastinolytic (35) activity. Although CTSL is located mainly in the endosomal/lysosomal compartment, ~10% is physiologically secreted and can be extracellularly activated (15). There, it is capable of processing ECM proteins such as fibronectin, laminin, elastin, and collagen types I, IV, and XVII (15, 34, 36–38). In turn, CTSL activity induces further ECM degradation by other proteases (35, 37). In vivo, the level of CTSL mRNA is related to tumor progression and metastatic potential, and this is thought to be related to the ability of CTSL to degrade ECM and basement membranes (16). In addition, it has been recently proposed that CTSL plays a role in ECM degradation during early mammary gland involution (19). Thus, the absence of CTSL would generate the accumulation of components of the ECM as it has been suggested for myocardium in CTSL KO mice (24) and observed in *nkt/nkt* heart (our unpublished results). In accordance, ECM components such as laminin, fibronectin, collagen I and IV were found to be increased in lymph nodes from *nkt/nkt* mice. Concomitantly, the percentage of lymph node T cells expressing high levels of  $\alpha_5$ ,  $\alpha_6$ , and  $\beta_1$  integrin chains was increased. However, in the spleen, no alterations in the level of ECM components or changes in the level of expression of  $\alpha_5$ ,  $\alpha_6$ , and  $\beta_1$  integrin chains in T cells could be detected.

ECM components have been shown to transduce survival signals through integrins (6, 7, 39, 40). It has also been demonstrated that ECM components promote the proliferation of T cells by signaling through integrins (9). Besides, different growth factors, chemokines and hormones have been shown to be associated with ECM (10–13), this association being an important factor in regulating not only their availability but also the cellular responsiveness (10, 12–14). Thus, it can be considered that increases in ECM components may increase the number of niches allowing the survival of an increased number of T (and B) cells in lymph nodes and also may favor cell proliferation. Increases in cell proliferation were detected in CD4<sup>+</sup> but not in CD8<sup>+</sup> lymph node T cells. The mechanisms underlying selective CD4<sup>+</sup> proliferation remain unknown. However several hypotheses can be proposed. Although homeostatic proliferation cannot be discarded it is difficult to reconcile with the presence of high numbers of CD8<sup>+</sup> cells in lymph nodes. Moreover, a significant percentage of CD4<sup>+</sup> cells express

Table IV. Increment of thymic export of CD8<sup>+</sup> thymocytes in *nkt/nkt* mice<sup>a</sup>

	Total CD8 <sup>+</sup> RTE	CD8 <sup>+</sup> RTE/SP CD8 <sup>+</sup>	Total CD4 <sup>+</sup> RTE	CD4 <sup>+</sup> RTE/SP CD4 <sup>+</sup>
<i>nkt/+</i>	4.1 × 10 <sup>5</sup> ± 0.9	0.05 ± 0.01	10.1 × 10 <sup>5</sup> ± 2.8	0.052 ± 0.028
<i>nkt/nkt</i>	11.2 × 10 <sup>5</sup> ± 2.8*	0.15 ± 0.03**	3.6 × 10 <sup>5</sup> ± 0.6*	0.066 ± 0.029

<sup>a</sup> FITC was injected intrathymically in *nkt/nkt* and *nkt/+* littermates; 24 h later, cells from lymph nodes, spleen, and thymus were stained with anti-CD4 and anti-CD8 and analyzed by FACS. RTE cells were identified as live-gated FITC<sup>+</sup> cells expressing either CD4 or CD8 in the periphery. Thymic export rate was calculated as the relation of the total number of CD8<sup>+</sup> RTE or CD4<sup>+</sup> RTE/the total number CD8<sup>+</sup> or CD4<sup>+</sup> simple positive thymocytes, respectively. Values represent mean number ± SD ( $n = 4$ ). \*,  $p < 0.05$ , \*\*,  $p < 0.001$ , compared to *nkt/+*. The experiment was performed six times with similar results.

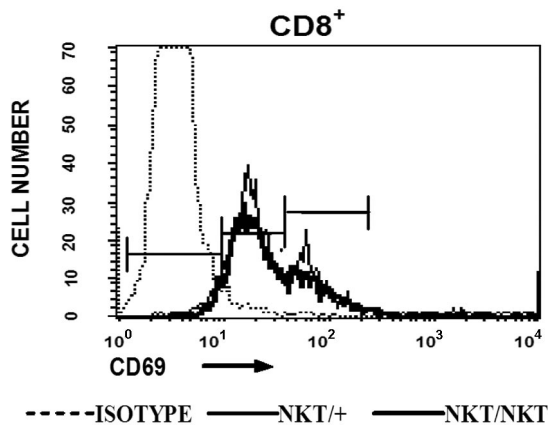


**FIGURE 8.** *nkt/nkt* mice show normal expression of CD69 on CD8<sup>+</sup> thymocytes. Expression of CD69 on CD8<sup>+</sup> thymocytes from *nkt/+* and *nkt/nkt* was analyzed by FACS. Histogram depicts representative results from three independent experiments.

CD69, an early marker of T cell activation which has not been observed in cells undergoing homeostatic proliferation (41). Neither can alterations in the recognition of self Ags in the periphery be discarded since it has been reported that CTSL KO mice display an altered repertoire in CD4<sup>+</sup> (22). Contrary to lymph nodes, the spleen—which show no alterations in ECM components and integrin chains levels—showed no changes in the total number or in the basal proliferative level of CD4<sup>+</sup> cells. Thus, it is possible that, in a situation of low thymic output of CD4<sup>+</sup> cells, increased ECM components in lymph nodes could lead to their proliferation.

Overall, these results suggest that the mutation in the *Ctsl* gene present in *nkt/nkt* mice leads to alterations in lymph node cell counts probably by causing increases in ECM components.

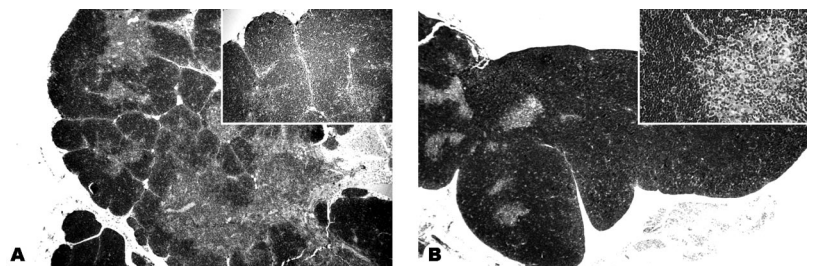
Immunohistochemical studies showed that *nkt/nkt* mice had important decreases in several components of thymic ECM such as laminin, fibronectin, and type I and IV collagens, both in the medulla and in the cortex. The regulatory mechanisms involved in the control of thymic ECM production and degradation are poorly understood (reviewed in Ref. 42). Although some metalloproteinases have been shown to be constitutively expressed in human thymus (43) and transcripts for metalloproteinase-9 have also been detected in fetal mouse thymocyte precursors (44), their role in the physiological breakdown of thymic ECM remains unclear. The possibility exists that in *nkt/nkt* mice, the lack of CTSL leads to increases in other proteases—as it has been recently shown for procathepsin D in the thyroid gland of CTSL<sup>-/-</sup> mice (25)—which could be responsible for ECM degradation. In contrast, different factors have been involved in the control of ECM production (45–47). In human thymic epithelial cells, insulin growth factor-1 (IGF-1) stimulates the expression of laminin and fibronectin, as well as their receptors VLA-5 and VLA-6 (46). It has been recently reported that CTSL-deficient fibroblasts show a decreased degradation of IGF binding protein-3 (IGFBP-3) (48). Limited proteol-

ysis of IGFBP from IGF/IGFBP complexes constitutes a central mechanism for the release of IGF from these complexes (49). Thus, a putative decrease in IGFBP degradation in the thymus could play a role in the decreased thymic ECM composition of *nkt/nkt* mice. However, we were not able to detect alterations in the levels of laminin 1, 2, and 5 and fibronectin mRNAs in the thymus of *nkt/nkt* mice (data not shown) nor in thymocyte expression of  $\alpha_6$ ,  $\alpha_5$ ,  $\alpha_4$ , and  $\beta_1$  integrin chains. Therefore, these results do not support a central role for alterations in the proteolysis of IGF/IGFBP complexes in the thymic decrease of ECM components. In contrast, in vitro studies have shown that thyroid hormones are able to enhance laminin and fibronectin as well as VLA-5 and VLA-6 expression in mouse and human thymic epithelial cells. CTSL has been proposed to be involved in the processing and solubilization of the prohormone thyroglobulin (47). In this sense, alterations in thyroid function could play a role in the thymic decrease of ECM in *nkt/nkt* mice.

Whatever the mechanisms involved, decreases in thymic ECM glycoproteins not only could greatly alter the availability and activity of different chemokines (13, 14), hormones, and growth factors (10, 11), but also could have effects on integrins/ligands interactions, thus influencing thymocyte development. Interactions between integrins displayed by thymocytes and ECM components, especially fibronectin and laminin, have been shown to strongly influence T cell differentiation/maturation possibly by stabilizing interactions between thymocytes and the epithelial components of the thymus (4–6, 50). The interaction of thymocyte integrins with their ECM ligands also leads to intracellular signaling (50). It has also been proposed that thymic ECM glycoproteins would constitute a macromolecular arrangement allowing differentiating thymocytes to migrate (51). Dysregulated ECM production/distribution correlates with alterations in intrathymic cell maturation and trafficking as recently shown in laminin  $\alpha_2$ -chain mutant *dy<sup>3k</sup>/dy<sup>3k</sup>* mice (52) and in experimental Chagas' disease (53). In the case of *dy<sup>3k</sup>/dy<sup>3k</sup>* mice, the lack of laminin 2 (merosin) is associated with a severe thymic atrophy resulting from apoptosis of double-positive (DP) cells. In vitro experiments suggested that the interaction of merosin with integrin  $\alpha_6\beta_1$  in the thymus is able to block the apoptosis of DP thymocytes. In contrast, during the course of *Trypanosoma cruzi* infection, a progressive increase in fibronectin and laminin expression correlates with increases in thymocyte migration ability; as a result, immature DP cells are found in the periphery of infected animals.

Herein, we show that in *nkt/nkt* mice, the decrease in thymic ECM components correlates with an increase both in the daily output of CD8<sup>+</sup> cells and in their thymic export rate. Taking into account that the total number of hemopoietic bone marrow cells is increased in mutant mice (our unpublished results), the high output of mature CD8<sup>+</sup> T cells could be related to increases in the entry of T cell precursors into the thymus. Alterations in thymocyte traffic and maturation could also be involved. Changes in thymocyte traffic could be recorded at least in the rate of emigration of CD8<sup>+</sup> cells. No differences in the percentage of CD8<sup>+</sup> SP thymocytes

**FIGURE 9.** *nkt/nkt* thymus shows alterations in the histological structure. *A*, Thymus from *nkt/+* mice showing classical histological pattern with two well-delimited compartments: cortex and medulla (H&E,  $\times 25$ ); *inset*, lobular pattern and cortex-medulla bound (H&E,  $\times 250$ ). *B*, *nkt/nkt* thymus with decreased medulla and enlarged cortex with less packed cells (H&E,  $\times 25$ );  $\times$ , cortex-medulla diffuse border (H&E,  $\times 250$ ).





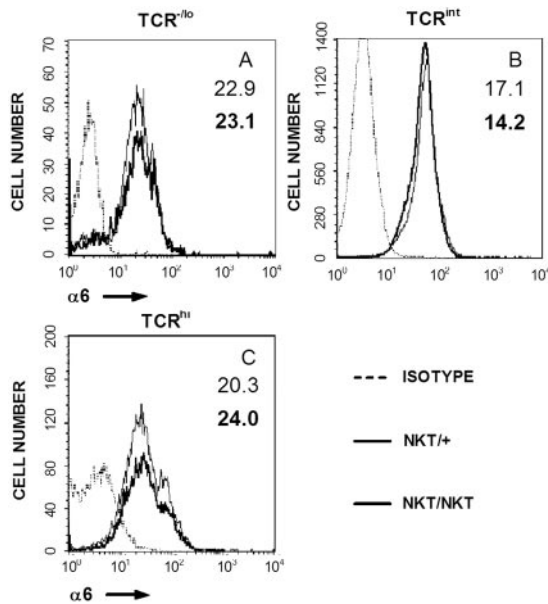


**FIGURE 10.** Expression of the  $\alpha_6$  integrin chain during thymocyte maturation in *nkt/nkt* mice. Expression of the integrin chain on electronically gated thymocytes expressing different levels of TCR (A, TCR<sup>-lo</sup>; B, TCR<sup>int</sup>; C, TCR<sup>hi</sup>) was analyzed by FACS. Percentages of  $\alpha_6^{\text{high}}$  are indicated for *nkt/+* (light) or *nkt/nkt* (bold). Histograms depict representative results from three independent experiments.

expressing CD69 high, intermediate, and negative levels were detected in the CD8 thymic compartment when *nkt/nkt* and control mice were compared. Although the mechanisms underlying the selective increased export of CD8<sup>+</sup> SP thymocytes remain unknown, our data suggest that changes in the speed of maturation and exit would include all the stages of CD8<sup>+</sup> SP thymocytes since neither diminution nor accumulation could be detected along all stages of their maturation. Finally, it is tempting to speculate that alterations in thymic ECM could also affect lineage commitment. The intracellular signaling pathways stimulated by integrin-ligand binding are shared by a number of other surface receptors expressed on thymocytes, including growth factor receptors, the TCR-CD3 complex, CD4 and CD8 (54). It has been reported that the intensity of signals appears to be crucial for positive selection and CD4/CD8 lineage commitment (55–59). Stronger and/or longer TCR signals may be required for CD4 than for CD8 lineage commitment (56–60). In addition, it has been shown that a strong MAPK signal is required for CD4<sup>+</sup> differentiation (61), and that blocking this signal favors CD8<sup>+</sup> production (61–63). Schmeissner et al. (64), using a mouse system that transgenically expresses a chimeric molecule shown to have dominant negative effects on integrin functions, suggested that integrin signaling is required for

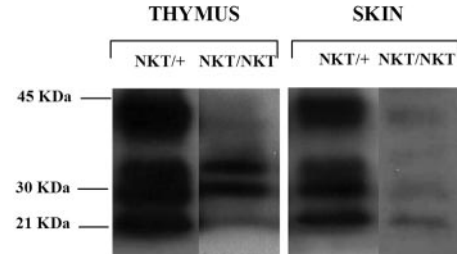


**FIGURE 11.** Positive CTSL expression in *nkt/nkt* mice. Lysates of thymus and skin from *nkt/+* and *nkt/nkt* mice were normalized to equal amounts of protein, separated on 15% SDS gels, and immunoblotted with an Ab against CTSL. Molecular mass markers are indicated in the left margins.

the generation of CD4<sup>+</sup> cells but is not essential for the production of CD8<sup>+</sup> cells. Moreover, the authors suggested that the disruption of integrin function leads to a shift from the CD4 to the CD8 lineage that correlates with an increased CD8:CD4 ratio in the spleen (64). Although integrin activation was not investigated in *nkt/nkt* mice, no alterations in the expression of  $\alpha_4$ ,  $\alpha_5$ ,  $\alpha_6$ , and  $\beta_1$  molecules during the different stages of thymocyte development could be detected. However, mutant mice showed a marked decrease in laminin, fibronectin, collagen I and IV thymic expression. Thus, in a scenario in which CD4<sup>+</sup>-positive selection is impaired, the possibility exists that thymocyte signaling through integrin-ECM interactions is decreased and that this could influence lineage commitment favoring a shift from the CD4<sup>+</sup> to the CD8<sup>+</sup> fate.

Benavides et al. (26) were not able to detect CTSL in the skin of *nkt/nkt* mice using the Ab M-19 from Santa Cruz Biotechnology, raised against a peptide mapping at the C terminus of the L chain of CTSL. The 118-bp deletion they described for CTSL in *nkt/nkt* mice involves the end of exon 6 and almost all of exon 7, sequences partially coding for the protein H and L chains. In accordance with the sequence reported (26), no C terminus of the L chain could be expected to be produced and therefore the amino acid sequence recognized by the M-19 Ab should be absent from a putative mutated form of CTSL. Results reported herein show that, although at a lower level, it has been possible to detect CTSL in thymus and skin from *nkt/nkt* mice using the AF1515 Ab (R&D Systems) directed to aa 18–334 in Western blot assays. Moreover, the immunohistochemical analysis of *nkt/nkt* tissues exhibited a very strong staining for CTSL (data not shown). Chauhan et al. (65) suggested that human CTSL lacking the 16 C-terminal amino acids is retained in the endoplasmic reticulum presumably because of its improper folding. Our results suggest that *nkt/nkt* mice express a mutated form of CTSL. The possibility exists that the presence of a mutated CTSL in *nkt/nkt* mice could lead to the appearance of phenotypic differences between KO and *nkt/nkt* mice. Therefore, it would be of interest to investigate which of the *nkt/*

Table V.  $\alpha_4$  and  $\alpha_5$  integrin chain expression as a function of TCR $\beta$  chain surface level in thymocytes from *nkt/nkt* or *nkt/+* mice<sup>a</sup>

	$\alpha_4$				$\alpha_5$			
	Low/int		High		Low/int		High	
	<i>nkt/+</i>	<i>nkt/nkt</i>	<i>nkt/+</i>	<i>nkt/nkt</i>	<i>nkt/+</i>	<i>nkt/nkt</i>	<i>nkt/+</i>	<i>nkt/nkt</i>
TCR <sup>-low</sup>	82.0 ± 3.6	74.8 ± 8.1	10.5 ± 4.2	11.7 ± 3.3	75.8 ± 2.6	71.9 ± 7.3	17.4 ± 1.6	16.8 ± 1.8
TCR <sup>int</sup>	88.6 ± 0.8	82.8 ± 4.7	8.0 ± 1.4	10.9 ± 1.4	61.6 ± 4.9	57.5 ± 5.7	36.3 ± 6.3	39.2 ± 5.1
TCR <sup>high</sup>	75.5 ± 2.9	68.3 ± 3.3	16.5 ± 4.7	22.2 ± 4.9	31.2 ± 3.9	26.1 ± 4.4	65.2 ± 5.0	70.8 ± 6.7

<sup>a</sup> Thymocytes from *nkt/nkt* and *nkt/+* littermates were stained with anti-TCR $\beta$  chain and anti-CD49d or anti-CD49e and analyzed by flow cytometry. Values represent the mean percentages of cells expressing low/intermediate or high levels of  $\alpha_4$  or  $\alpha_5$  integrin chains ± SD ( $n = 4$ ) within electronically gated populations expressing different levels of TCR. The experiment was performed three times with similar results.

*nkt* phenotypes described herein are also shared by CTSL KO mice, to determine whether the presence of a mutated form of CTSL plays a role in some of the alterations observed.

To our knowledge, these results demonstrate by the first time that a mutation in the *Ctsl* gene is able to affect the levels of ECM components in lymphoid organs. Moreover, the opposite effects registered in thymic and lymph node ECM in CTSL mutant mice further underline the variability of CTSL functions among different organs. Results reported herein also show that the *nkt* mutation broadly affects the immune system, influencing the thymic output of CD8<sup>+</sup> cells and the regulation of the number of T cells in the periphery. We postulate that these influences would be a consequence of alterations in ECM expression.

## Acknowledgments

We thank Dr. C. D. Pasqualini for helpful discussions. We are grateful to Antonio Morales, Julio Tejada, and Juan Portaluppi for efficient technical assistance.

## Disclosures

The authors have no financial conflict of interest.

## References

- Berrith, S., W. Savino, and S. Cohen. 1985. Extracellular matrix of the human thymus: immunofluorescence studies on frozen sections and cultured epithelial cells. *J. Histochem. Cytochem.* 33: 655–664.
- Lannes-Vieira, J., M. Dardenne, and W. Savino. 1991. Extracellular matrix components of the mouse thymus microenvironment. Ontogenetic studies and modulation by glucocorticoid hormones. *J. Histochem. Cytochem.* 39:1539–1546.
- Castaños-Velez, E., P. Biberfeld, and M. Patarroyo. 1995. Extracellular matrix proteins and integrin receptors in reactive and non-reactive lymph nodes. *Immunology* 86: 270–278.
- Utsumi K., M. Sawada, S. Narumiya, J. Nagamine, T. Sakata, S. Iwagami, Y. Kita, H. Teraoka, H. Hirano, M. Ogata, et al. 1991. Adhesion of immature thymocytes to thymic stromal cells through fibronectin molecule and its significance for the induction of thymocyte differentiation. *Proc. Natl. Acad. Sci. USA* 88: 5685–5689.
- Salomon, D. R., C. F. Mojciak, A. C. Chang, S. Wadsworth, D. H. Adams, J. E. Coligan, and E. M. Shevach. 1994. Constitutive activation of integrin  $\alpha_4\beta_1$  defines a unique stage of human thymocytes development. *J. Exp. Med.* 179: 1573–1584.
- Chang, A. C., D. R. Salomon, S. Wadsworth, M. J. Ilong, C. F. Mojciak, S. Otto, E. M. Shevach, and J. E. Coligan. 1995.  $\alpha_3\beta_1$  and  $\alpha_6\beta_1$  integrins mediate laminin/merosin binding and function as costimulatory molecules for human thymocyte proliferation. *J. Immunol.* 154: 500–510.
- Matsuyama, T., A. Yamada, J. Kay, K. M. Yamada, S. K. Akiyama, S. F. Schlossman, and C. Morimoto. 1989. Activation of CD4 cells by fibronectin and anti-CD3 antibodies: a synergistic effect mediated by the VLA-5 fibronectin receptor complex. *J. Exp. Med.* 170: 1133–1148.
- Adler, B., S. Ashkar, H. Cantor, and G. F. Weber. 2001. Costimulation by extracellular matrix proteins determines the response to TCR ligation. *Cell. Immunol.* 210: 30–40.
- Tschoetschel, U., J. Schwing, S. Frosch, E. Schmitt, D. Schuppan, and A. K. Reske-Kunz. 1997. Modulation of proliferation and lymphokine secretion of murine CD4F T cells and cloned Th1 cells by proteins of the extracellular matrix. *Int. Immunol.* 9: 147–159.
- Jones, J. L., A. Gockerman, W. H. Jr. Busby, C. Camacho-Hubner, and D. R. Clemmons. 1993. Extracellular matrix contains insulin-like growth factor binding protein-5: potentiation of the effects of IGF-I. *J. Cell Biol.* 121: 679–687.
- Taipale, J., K. Miyazono, C. H. Heldin, and J. Keski-Oja. 1994. Latent transforming growth factor- $\beta$ 1 associates to fibroblast extracellular matrix via latent TGF- $\beta$  binding protein. *J. Cell Biol.* 124: 171–181.
- Rich, S., N. Van Nood, and H. M. Lee. 1996. Role of  $\alpha_5\beta_1$  integrin in TGF- $\beta$ 1-costimulated CD8<sup>+</sup> T cell growth and apoptosis. *J. Immunol.* 157: 2916–2923.
- Pelletier, A. J., L. J. W. van der Laan, P. Hildbrand, M. A. Sian, D. A. Thompson, P. E. Dawson, B. E. Torbett, and D. R. Salomon. 2000. Presentation of chemokine SDF-1 $\alpha$  by fibronectin mediates directed migration of T cells. *Blood* 96: 2682–2690.
- Yanagawa, Y., K. Iwabuchi, and K. Onoé. 2001. Enhancement of stromal cell-derived factor-1 $\alpha$ -induced chemotaxis for CD4/8 double-positive thymocytes by fibronectin and laminin in mice. *Immunology* 104: 43–49.
- Felbor, U., I. Dreier, R. A. Bryant, H. L. Ploegh, B. R. Olsen, and W. Mothes. 2000. Secreted cathepsin L generates endostatin from collagen XVIII. *EMBO J.* 19: 1187–1194.
- Lah, T. T., and J. Kos. 1998. Cysteine proteinases in cancer progression and their clinical relevance for prognosis. *Biol. Chem.* 379: 125–130.
- Afonso, S., L. Romagnano, and B. Babiarz. 1997. The expression and function of cystatin C and cathepsin B and cathepsin L during mouse embryo implantation and placentation. *Development* 124: 3415–3425.
- Roth, W., J. Deussing, V. A. Botchkarev, M. Pauly-Evers, P. Saftig, A. Hafner, P. Schmidt, W. Schmahl, J. Scherer, I. Anton-Lamprecht, et al. 2000. Cathepsin L deficiency as molecular defect of *furless*: hyperproliferation of keratinocytes and perturbation of hair follicle cycling. *FASEB J.* 14: 2075–2086.
- Burke, M. A., D. Hutter, R. P. Reshamwala, and J. E. Knepper. 2003. Cathepsin L play an active role in involution of the mouse mammary gland. *Dev. Dyn.* 227: 315–322.
- Turk, V., B. Turk, and D. Turk. 2001. Lysosomal cysteine proteases: facts and opportunities. *EMBO J.* 20: 4629–4633.
- Nakagawa, T., W. Roth, P. Wong, A. Nelson, A. Farr, J. Deussing, J. A. Villadangos, H. Ploegh, C. Peters, and A. Y. Rudensky. 1998. Cathepsin L: critical role in li degradation and CD4 T cell selection in the thymus. *Science* 280: 450–453.
- Honey, K., T. Nakagawa, C. Peters, and A. Rudensky. 2002. Cathepsin L regulates CD4<sup>+</sup> T cell selection independently of its effect on invariant chain: a role in the generation of positively selecting peptide ligands. *J. Exp. Med.* 195: 1349–1358.
- Tobin, D. J., K. Foitzik, T. Reinheckel, L. Mecklenburg, V. A. Botchkarev, C. Peters, and R. Paus. 2002. The lysosomal protease cathepsin L is an important regulator of keratinocyte and melanocyte differentiation during hair follicle morphogenesis and cycling. *Am. J. Pathol.* 160: 1807–1821.
- Stypmann, J., K. Glaser, W. Roth, D. Tobin, I. Petermann, R. Matthias, G. Monnig, W. Haverkamp, G. Breithardt, W. Schmahl, et al. 2002. Dilated cardiomyopathy in mice deficient for the lysosomal cysteine peptidase cathepsin L. *Proc. Natl. Acad. Sci. USA* 99: 6234–6239.
- Friedrichs, B., C. Tepel, T. Reinheckel, J. Deussing, K. von Figura, V. Herzog, C. Peters, P. Saftig, and K. Brix. 2003. Thyroid functions of mouse cathepsins B, K, and L. *J. Clin. Invest.* 111: 1733–1745.
- Benavides, F., A. Venables, H. Poetschke Klug, E. Glasscock, A. Rudensky, M. Gómez, N. Martín Palenzuela, J. L. Guénet, E. R. Richie, and C. Conti. 2001. The CD4 T cell-deficient mouse mutation *nackt* (*nkt*) involves a deletion in the cathepsin L (*Ctsl*) gene. *Immunogenetics* 53: 233–342.
- Nepomnaschy, I., M. G. Lombardi, P. Beckinshtein, P. Berguer, V. Francisco, J. De Almeida, V. Buggiano, C. D. Pasqualini, and I. Piazzon. 2000. Alterations in positive selection in the thymus of CD4 deficient *nackt* mice. *Scand. J. Immunol.* 52: 555–562.
- Benavides, F., M. Giordano, L. Fiette, A. L. Bueno Brunialti, N. Martín Palenzuela, S. Vanzulli, P. Baldi, R. Schmidt, C. D. Pasqualini, and J. Guenet. 1999. *Nackt* (*nkt*), a new hair loss mutation of the mouse with associated CD4 deficiency. *Immunogenetics* 49: 413–419.
- Piazzon, I., A. Goldman, S. Torello, I. Nepomnaschy, A. Deroche, and G. Dran. 1994. Transmission of an Mls-1a-like superantigen to BALB/c mice by foster-nursing on F1 Mls-1 bxa mothers: sex-influenced onset of clonal deletion. *J. Immunol.* 153: 1553–1562.
- Mundel, P., H. W. Heid, T. M. Mundel, M. Kruger, J. Reiser, and W. Kriz. 1997. Synaptodin: an actin-associated protein in telencephalic dendrites and renal podocytes. *J. Cell Biol.* 139: 193–204.
- Berzins, S. P., D. L. Godfrey, J. F. A. P. Miller, and R. L. Boyd. 1999. A central role for thymic emigrants in peripheral T cell homeostasis. *Proc. Natl. Acad. Sci. USA* 96: 9787–9791.
- Bendelac, A., P. Matzinger, A. Seder, W. E. Paul, and R. H. Schwartz. 1992. Activation events during thymic selection. *J. Exp. Med.* 175: 731–42.
- Feng, C., K. J. Woodside, B. A. Vance, D. El-Khoury, M. Canelles, J. Lee, R. Gress, B. J. Fowlkes, E. W. Shores, and P. E. Love. 2002. A potential role for CD69 in thymocyte emigration. *Int. Immunol.* 14: 535–544.
- Maciewicz, R. A., and D. J. Etherington. 1998. A comparison of four cathepsins (B, L, N and S) with collagenolytic activity from rabbit spleen. *Biochem. J.* 256: 433–440.
- Chapman, H. A. Jr., J. S. Munger, and G. P. Shi. 1994. The role of thiol proteases in tissue injury and remodeling. *Am. J. Respir. Crit. Care Med.* 150: S155–S159.
- Blondeau, X., S. L. Vidmar, I. Emod, M. Pagano, V. Turk, and V. Keil-Douha. 1993. Generation of matrix-degrading proteolytic system from fibronectin by cathepsins B, G, H, and L. *Biol. Chem. Hoppe-Seyler* 374: 651–656.
- Guinec, N., V. Dalet-Fumeron, and M. Pagano. 1993. "In vitro" study of basement membrane degradation by the cysteine proteinases, cathepsins B, B-like, and L. Digestion of collagen IV, laminin, fibronectin, and release of gelatinase activities from basement membrane fibronectin. *Biol. Chem. Hoppe-Seyler* 374: 1135–1146.
- Schenepel J., and H. Tschesche. 2000. The proteolytic activity of the recombinant cryptic fibronectin type IV collagenase from *E. coli* expression. *J. Protein Chem.* 19: 685–692.
- Matter, M. L., and E. Ruoslahti. 2001. A signaling pathway from the  $\alpha_5\beta_1$  and  $\alpha_v\beta_3$  integrins that elevates *bcl-2* transcription. *J. Biol. Chem.* 276: 27757–27763.
- Gendron, S., J. Couture, and F. Aoudjit. 2003. Integrin  $\alpha_2\beta_1$  inhibits Fas-mediated apoptosis in T lymphocytes by protein phosphatase 2A-dependent activation of the MAPK/ERK pathway. *J. Biol. Chem.* 278: 48633–48643.
- Clarke S. R., and A. Y. Rudensky. 2000. Survival and homeostatic proliferation of naive peripheral CD4<sup>+</sup> T cells in the absence of self peptide: MHC complexes. *J. Immunol.* 165: 2458–2464.
- Savino W., D. A. Mendes-da-Cruz, J. S. Silva, M. Dardenne, and V. Cotta-de-Almeida. 2002. Intrathymic T-cell migration: a combinatorial interplay of extracellular matrix and chemokines? *Trends Immunol.* 23: 305–313.
- Kondo, K., H. Kinoshita, H. Ishikura, T. Miyoshi, T. Hirose, Y. Matsumori, and Y. Monden. 2001. Activation of matrix metalloproteinase-2 is correlated with invasiveness in thymic epithelial tumors. *J. Surg. Oncol.* 76: 169–175.
- Wilkinson, B., J. J. T. Owen, and E. J. Jenkinson. 1999. Factor regulating stem cell recruitment to the fetal thymus. *J. Immunol.* 162: 3873–3781.

45. Savino W., and M. Dardenne. 2000. Neuroendocrine control of thymus physiology. *Endocr. Rev.* 21: 412–413.
46. de Mello Coelho, V., D. M. Villa-Verde, D. A. Farias-de-Oliveira, J. M. Brito, M. Dardenne, and W. Savino. 2002. Functional insulin-like growth factor-1/insulin-like growth factor-1 receptor-mediated circuit in human and murine thymic epithelial cells. *Neuroendocrinology* 75: 139–150.
47. Ribeiro-Carvalho, M. M., D. A. Farias-de-Oliveira, D. M. Villa-Verde, and W. Savino. 2002–2003. Triiodothyronine modulates extracellular matrix-mediated interactions between thymocytes and thymic microenvironmental cells. *Neuroimmunomodulation* 10: 142–152.
48. Zwad, O., B. Kubler, W. Roth, J. G. Scharf, P. Saftig, C. Peters, and T. Bräulke. 2002. Decreased intracellular degradation of insulin-like growth factor binding protein-3 in cathepsin L-deficient fibroblast. *FEBS Lett.* 510: 211–215.
49. Rudman, S. M., M. P. Philpott, G. A. Thomas, and T. Kealey. 1997. The role of IGF-I in human skin and its appendages: morphogen as well as mitogen? *J. Invest. Dermatol.* 109: 770–777.
50. Wadsworth, S., M. J. Halvorson, and J. E. Coligan. 1992. Developmentally regulated expression of the  $\beta_4$  integrin on immature mouse thymocytes. *J. Immunol.* 149: 421–428.
51. Savino W., S. R. Dalmau, and V. C. Dealmeida. 2000. Role of extracellular matrix-mediated interactions in thymocyte migration. *Dev. Immunol.* 7: 279–291.
52. Iwao, M., S. Fukuda, T. Harada, K. Tsujikawa, H. Yagita, C. Hiramane, Y. Miyagoe, S. Takeda, and H. Yamamoto. 2000. Interaction of merosin (laminin 2) with very late activation antigen-6 is necessary for the survival of CD4<sup>+</sup>CD8<sup>+</sup> immature thymocytes. *Immunology* 99: 481–488.
53. Cotta-de-Almeida, V., A. Bonomo, D. A. Mendez-da-Cruz, I. Riederer, J. de Meis, K. R. F. Lima-Quaresma, A. Vieira-de-Abreu, D. M. S. Villa-Verde, and W. Savino. 2003. *Trypanosoma cruzi* infection modulates intrathymic contents of extracellular matrix ligands and receptors and alters thymocyte migration. *Eur. J. Immunol.* 33: 2439–2448.
54. Miyamoto, Y. J., B. F. Andruss, J. S. Mitchell, M. J. Billard, and B. W. McIntyre. 2003. Diverse roles of integrins in human T lymphocyte biology. *Immunol. Res.* 27: 71–84.
55. Matechak, E. O., N. Killeen, S. M. Hedrick, and B. J. Fowlkes. 1996. MHC class II-specific T cells can develop in the CD8 lineage when CD4 is absent. *Immunity* 4: 337–347.
56. Watanabe, N., H. Arase, M. Onodera, P. S. Ohashi, and T. Saito. 2000. The quantity of TCR signal determines positive selection and lineage commitment of T cells. *J. Immunol.* 165: 6252–6261.
57. Hernandez-Hoyos, G., S. J. Sohn, E.V. Rothenberg, and J. Alberola-Lla. 2000. Lck activity controls CD4/CD8 T cell lineage commitment. *Immunity* 12: 313–322.
58. Legname, G., B. Seddon, M. Lovatt, P. Tomlinson, N. Sarner, M. Tolaini, K. Williams, T. Norton, D. Kioussis, and R. Zamoyska. 2000. Inducible expression of a p56<sup>Lck</sup> transgene reveals a central role for Lck in the differentiation of CD4 SP thymocytes. *Immunity* 12: 537–546.
59. Adachi, S., and M. Iwata. 2002. Duration of calcineurin and Erk signals regulates CD4/CD8 lineage commitment of thymocytes. *Cell. Immunol.* 215: 45–53.
60. Yasutomo, K., C. Doyle, L. Miele, and R. N. Germain. 2000. The duration of antigen receptor signaling determines CD4<sup>+</sup> versus CD8<sup>+</sup> T-cell lineage fate. *Nature* 404: 506–510.
61. Sharp, L. L., D. A. Schwartz, C. M. Bott, C. J. Marshall, and S. M. Hedrick. 1997. The influence of the MAPK pathway on the T cell lineage commitment. *Immunity* 7: 609–618.
62. Bommhardt, U., M. A. Basson, U. Krummrei, and R. Zamoyska. 1999. Activation of the extracellular signal-related kinase/mitogen-activated protein kinase pathway discriminates CD4 versus CD8 lineage. *J. Immunol.* 163: 715–722.
63. Sharp L. L., and S. M. Hedrick. 1999. Commitment to the CD4 lineage mediated by extracellular signal-related kinase mitogen-activated protein kinase and *lck* signaling. *J. Immunol.* 163: 6598–6605.
64. Schmeissner, P. J., H. Xie, L. B. Smilenov, F. Shu, and E. E. Marcantonio. 2001. Integrin functions play a key role in the differentiation of thymocytes in vivo. *J. Immunol.* 167: 3715–3724.
65. Chauhan, S. S., D. Ray, S. E. Kane., M. C. Willingham, and M. M. Gottesman. 1998. Involvement of carboxy-terminal amino acids in secretion of human lysosomal protease cathepsin L. *Biochemistry* 37: 8584–8594.